AN INVERSE TONE MAPPING OPERATION WITH TWO INTEGER DATA FOR HDR IMAGES

Toshiyuki DOBASHI[⋆] *Masahiro IWAHASHI*[†] *Hitoshi KIYA*[⋆]

[⋆] Tokyo Metropolitan University, Tokyo, Japan
[†] Nagaoka University of Technology, Niigata, Japan

ABSTRACT

This paper proposes an inverse tone mapping operation (ITMO) for HDR images with low computational cost. An ITMO generates a high dynamic range (HDR) image from a low dynamic range (LDR) image. Since HDR images are generally expressed in a floating-point data format, an ITMO also deals with floating-point arithmetic. As a result, conventional ITMOs require high computational cost. There are many research works to reduce a computational cost in the TMOs. However, most of them are not for inverse TMO, but for forward TMO which generates an LDR image from an HDR image. To reduce a computational cost, the proposed method treats a floating-point number as two 8-bit integer numbers which correspond to an exponent part and a mantissa part, and applies inverse tone mapping to these integer numbers separately. Moreover, the method can conduct all calculations in the ITMO with only fixed-point arithmetic. The experimental results show the proposed method with fixed-point arithmetic is 6.86 times faster than the conventional method with floating-point arithmetic.

***Index Terms*—** High dynamic range, Tone mapping, Fixed-point

1. INTRODUCTION

High dynamic range (HDR) imaging is diffusing in many fields: photography, computer graphics, surveillance camera, HDR video, and more. These images have a high resolution of pixel values, i.e., numerous pixel tones. Compared with the current standard for low dynamic range (LDR) images, which are expressed in 8 bits, HDR images have an extremely long bit depth and high dynamic range of pixel values. To fully utilize this dynamic range under limited memory space, the pixel values are expressed as floating-point data, such as in OpenEXR [1], RGBE [2], or IEEE754 [3] format. However, display devices which can express the pixel values of HDR images are not popular yet. Therefore, the importance of a tone mapping operation (TMO) which generates an LDR image from an HDR image by compressing its dynamic range has been growing.

Various research works on TMOs have so far been done [4–19]. These are focused on quality of tone mapped images [4–8], compression techniques [9–11], and reducing a computational cost [12–19].

On the other hand, an inverse TMO (ITMO) is also attracting attention, recently. The ITMOs reconstruct HDR images from LDR ones, and have various important applications such as estimating HDR images [20–24] and multilayer coding [25–28]. Most of research works of the ITMOs are focused on generating a high-quality HDR image [20–24]. However, the existing ITMOs require data-depended calculations that have high computational cost. Specially, real-time processing such as HDR video or HDR TV, requires speeding-up of computing. Therefore, reducing computational cost regarding an ITMO is an important issue.

For these reasons, the proposed method considers to reduce the computational cost in the ITMO. The method is composed of 2 steps. First, the method treats a floating-point number in the ITMO process as two 8-bit integer numbers, which correspond to a exponent part and a mantissa part, and applies tone mapping to these integer numbers separately. Then, the method can be implemented with fixed-point arithmetic. Using 8-bit integer data facilitates executing calculations with fixed-point arithmetic because it eases the limitation of the bit length. Fixed-point arithmetic is often utilized in embedded systems because of the advantages such as low-power consumption, the small circuit size and high-speed computing [29, 30]. Therefore, the method can be processed at high-speed on the embedded systems, which have a low-performance processor without a floating-point unit (FPU).

The experimental results confirmed that the proposed method reduces the computational cost, and keeps the quality of generated HDR images, compared to the conventional method with floating-point arithmetic.

2. PRELIMINARIES

The conventional TMO and its inverse operation (ITMO) are described in this section.

2.1. Forward Tone Mapping Operation

A TMO generates an LDR image from an HDR image by compressing its dynamic range. There are two types of a TMO: global tone mapping and local tone mapping, this paper deals with global tone mapping. A procedure of the Reinhard's "Photographic Tone Reproduction" which is one of the well-known global TMOs [4] is described in this section.

First, the world luminance $L_w(p)$ of the HDR image is calculated from RGB pixel values of the HDR image,

$$L_w(p) = 0.27R(p) + 0.67G(p) + 0.06B(p), \tag{1}$$

where $R(p), G(p)$, and $B(p)$ are floating-point RGB pixel values at located p of the HDR image, respectively.

Next, the geometric mean $\bar{L}_w$ of the world luminance $L_w(p)$ is calculated as follows

$$\bar{L}_w = \exp\left(\frac{1}{N}\sum_p \log_e\left(L_w(p)\right)\right), \tag{2}$$

where N is the total number of pixels in the input HDR image.

Then, the scaled luminance $L(p)$ is calculated as

$$L(p) = k \cdot \frac{L_w(p)}{\bar{L}_w}, \tag{3}$$

where $k \in [0, 1]$ is the parameter called "key value".

Next, the display luminance $L_d(p)$ is calculated using a tone mapping function $y()$ as follows

$$L_d(p) = y(L(p)). \tag{4}$$

The Reinhard's global operator [4] which is one of the well-known tone mapping functions is defined as

$$y_{\text{Reinhard}}(L(p)) = \frac{L(p)}{1 + L(p)}. \tag{5}$$

Finally, the floating-point pixel values $C_F(p)$ of the LDR image is calculated as follows

$$C_F(p) = L_d(p) \cdot \frac{C(p)}{L_w(p)}, \tag{6}$$

where $C(p) \in \{R(p), G(p), B(p)\}$ is the floating-point RGB value of the input HDR image,
and $C_F(p) \in \{R_F(p), G_F(p), B_F(p)\}$.

The 24-bit color RGB values $C_I(p)$ of the LDR image is derived from

$$C_I(p) = \text{round}\left(C_F(p) \cdot 255\right), \tag{7}$$

where round(x) rounds x to its nearest integer value, and $C_I(p) \in \{R_I(p), G_I(p), B_I(p)\}$.

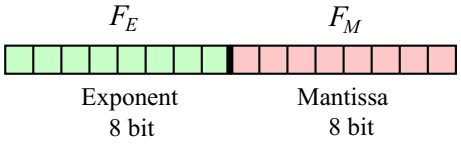

Fig. 1. The bit allocation of the proposed intermediate format.

2.2. Inverse Tone Mapping Operation

This section introduces the inverse operation of "Photographic Tone Reproduction" described in [24]. It is processed following procedure.

First, $L'_d(p)$ is calculated from RGB pixel values of the LDR image,

$$L'_d(p) = (0.27R_I(p) + 0.67G_I(p) + 0.06B_I(p)) \cdot \frac{1}{255}, \tag{8}$$

Next, the world luminance $L'_w(p)$ is calculated as

$$L'_w(p) = \frac{\bar{L}_w}{k} \cdot L(p) = \frac{\bar{L}_w}{k} \cdot \frac{L'_d(p)}{1 - L'_d(p)}, \tag{9}$$

Finally, the color RGB values $C'(p)$ of the HDR image is derived from

$$C'(p) = \frac{L'_w(p)}{L'_d(p)} \cdot C_F(p) = \frac{L'_w(p)}{L'_d(p)} \cdot \frac{C_I(p)}{255}. \tag{10}$$

In above processes, floating-point arithmetic and floating-point data are needed to obtain an HDR image expressed in floating-point. Therefore, large computational cost is required.

3. PROPOSED INVERSE TMO

3.1. Intermediate Format

The proposed ITMO generates an HDR image expressed in proposed intermediate format from an LDR image. The intermediate format is then converted into various HDR image formats such as OpenEXR [1], RGBE [2], and IEEE754 [3]. That is, the method is an unified operation which does not depend on HDR image formats. Figure 1 shows the bit allocation of the intermediate format. This format has 8-bit exponent part and 8-bit mantissa part for each color. The encode functions which yield the exponent part F_E and the mantissa part F_M of each RGB channel F are defined as

$$F_E = \lceil \log_2 F + 128 \rceil, \tag{11}$$

$$F_M = \left\lfloor F \cdot 2^{136 - F_E} \right\rfloor, \tag{12}$$

where $\lceil x \rceil$ rounds x to the nearest integer greater than or equal to x, and $\lfloor x \rfloor$ rounds x to the nearest integer less than or equal to x. On the other hand, the decode function which yields the original RGB value from the intermediate format is defined as

$$F = (F_M + 0.5) \cdot 2^{F_E - 136}. \tag{13}$$

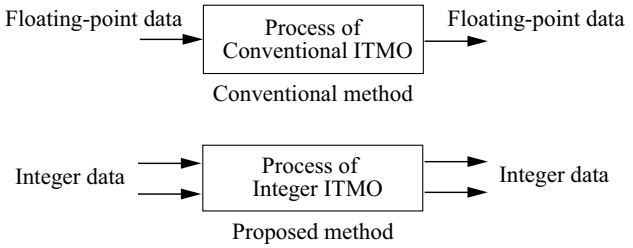

Fig. 2. The difference between the conventional method and the proposed integer ITMO.

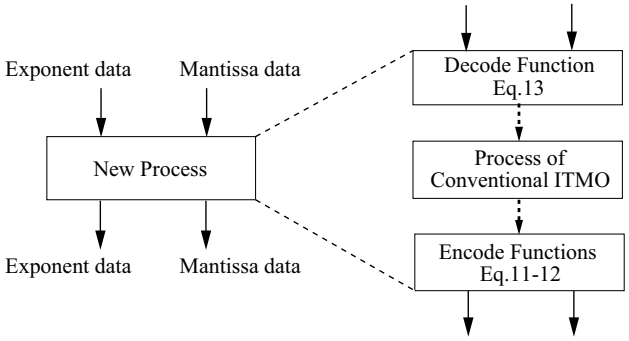

Fig. 3. A new process defined in the proposed integer ITMO.

3.2. Integer ITMO

The proposed method constructs the integer ITMO based on the integer TMO technique [12–14, 18]. The integer ITMO is defined as the ITMO which is implemented with integer input and integer output. Figure 2 shows the difference between the conventional method and the integer ITMO. The integer ITMO defines new processes and replaces each tone mapping process by them. These new processes are composite functions shown in Figure 3. In the proposed ITMO, the numerical range in the processes is significantly reduced because the exponent part and the mantissa part are separated as two integer numbers. Note that this technique of the integer ITMO works well by using the proposed intermediate format. The technique does not work well for the IEEE754 format because it has denormalized numbers as well as the OpenEXR [13].

The proposed integer ITMO is processed following procedure.

First, the exponent part $L_{d_E}(p)$ and the mantissa part $L_{d_M}(p)$ of the display luminance $L'_d(p)$ is calculated as

$$L_{d_E}(p) = \lceil \log_2 L_d(p) + 128 \rceil, \tag{14}$$

$$L_{d_M}(p) = \left\lfloor L_d(p) \cdot 2^{136 - L_{d_E}(p)} \right\rfloor, \tag{15}$$

$$L_d(p) = (0.27R_I(p) + 0.67G_I(p) + 0.06B_I(p)) \cdot \frac{1}{255}, \tag{16}$$

where $0 \leq L_{d_E}(p) \leq 255, 0 \leq L_{d_M}(p) \leq 255$.

Next, the method calculates the exponent part $L_{w_E}(p)$ and the mantissa part $L_{w_M}(p)$ of the world luminance $L'_w(p)$. This calculation depends on inverse tone mapping functions. Here, the inverse tone mapping function of Eq. (9) is used as an example,

$$FL_w(p) = \frac{L_{d_M}(p) + 0.5}{2^{136 - L_{d_E}(p)} - L_{d_M}(p) + 0.5} \cdot \frac{\bar{L}_w}{k}, \tag{17}$$

$$L_{w_E}(p) = \lceil \log_2 FL_w(p) + 128 \rceil, \tag{18}$$

$$L_{w_M}(p) = \left\lfloor FL_w(p) \cdot 2^{136 - L_{w_E}(p)} \right\rfloor, \tag{19}$$

where $0 \leq L_{w_E}(p) \leq 255$ and $0 \leq L_{w_M}(p) \leq 255$.

Then, the exponent part $C_E(p)$ and the mantissa part $C_M(p)$ of the HDR image expressed in the intermediate format are derived as

$$FC(p) = \frac{L_{w_M}(p) + 0.5}{L_{d_M}(p) + 0.5} \cdot \frac{C_I(p)}{255}, \tag{20}$$

$$C_E(p) = \lceil \log_2 FC(p) + L_{w_E}(p) - L_{d_E}(p) + 128 \rceil, \tag{21}$$

$$C_M(p) = \left\lfloor FC(p) \cdot 2^{136 - C_E(p) + L_{w_E}(p) - L_{d_E}(p)} \right\rfloor. \tag{22}$$

where $0 \leq C_E(p) \leq 255, 0 \leq C_M(p) \leq 255$.

Finally, the desired format of the HDR image can be obtained with the decode function in Eq. (13).

In the above processes, the input and output data of each calculation are all 8-bit integer data. The next section describes fixed-point implementation of the method.

3.3. Fixed-Point Implementation

In the integer ITMO, all data are converted to 8-bit integer, and the numerical range of above calculations are significantly reduced. As a result, the proposed method implements integer ITMO with fixed-point arithmetic to reduce the computational cost.

Most of equations can be calculated with fixed-point arithmetic because each variable is expressed in 8-bit integer. Nevertheless, Eq. (17) is difficult to be calculated without floating-point arithmetic because the range of value of the denominator can be very wide. Because of this, the method deforms Eq. (17) as follows

$$FL_w(p) = \frac{1}{\frac{2^{136 - L_{d_E}(p)}}{L_{d_M}(p) + 0.5} - 1} \cdot \frac{\bar{L}_w}{k}. \tag{23}$$

If the power of 2 in the denominator $(136 - L_{d_E}(p))$ is large value, 1 in the denominator can be ignored. Therefore, it is approximated as

$$FL_w(p) \approx \frac{1}{\frac{2^{136 - L_{d_E}(p)}}{L_{d_M}(p) + 0.5}} \cdot \frac{\bar{L}_w}{k} \tag{24}$$

$$= (L_{d_M}(p) + 0.5) \cdot \frac{\bar{L}_w}{k} \cdot 2^{-(136 - L_{d_E}(p))}, \tag{25}$$

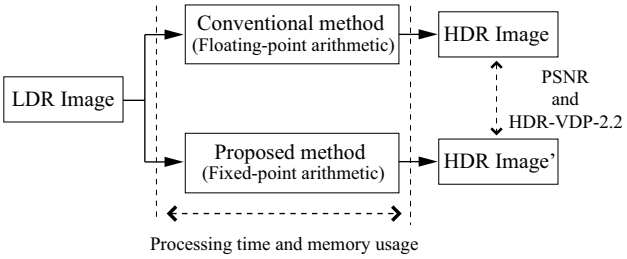

Fig. 4. The block diagram of the experiments.

Table 1. The conditions in the experiments.

	Arithmetic	Data
Proposed	32-bit Fixed-point	8-bit Integer
Conventional	64-bit Floating-point	64-bit Floating-point

therefore

$$L_{w_E}(p) = \left\lceil \log_2(L_{d_M}(p) + 0.5 \cdot \frac{\bar{L}_w}{k}) + L_{d_E}(p) - 8 \right\rceil, \tag{26}$$

$$L_{w_M}(p) = \left\lfloor (L_{d_M}(p) + 0.5) \cdot \frac{\bar{L}_w}{k} \cdot 2^{L_{d_E}(p) - L_{w_E}(p)} \right\rfloor. \tag{27}$$

The condition of this approximation depends on available bit length. In this paper, 32bit processor is used, and the approximation is performed when $(136 - L_{d_E}(p)) > 22$.

The method can calculate all equations of the ITMO with only fixed-point arithmetic using this approximation. The next section shows the effect of the proposed method.

4. EXPERIMENTAL RESULTS

The computational cost of the proposed method is reduced by using fixed-point arithmetic instead of floating-point arithmetic. However, errors can occur by fixed-point arithmetic. To confirm the efficacy of the proposed method and the errors involved with it, the experiments were carried out. These experiments consist of image quality assesment and evaluation of resource consumption. Figure 4 shows the block diagram of these experiments. The conventional method in this experiment is [24], which was described in Section 2.2. Both the proposed method and the conventional method [24] were implemented in C-language. Table 1 shows that condition of this experiment.

4.1. Generated HDR Image Quality

This experiment applied the ITMOs for LDR images using the proposed method and the conventional method [24], and measured the modified PSNR [31] and the HDR-VDP-2.2 [32] of the generated HDR images. This experiment was carried out for 32 LDR images which generated with the Reinhard's global TMO [4]. The HDR images $I_{\mathrm{HDR}}(p)$ and $I'_{\mathrm{HDR}}(p)$ are given by

$$I_{\mathrm{HDR}}(p) = \mathrm{IT_a}[I_{\mathrm{LDR}}(p)], \tag{28}$$

$$I'_{\mathrm{HDR}}(p) = \mathrm{IT_b}[I_{\mathrm{LDR}}(p)], \tag{29}$$

where $I_{\mathrm{LDR}}(p)$ is an input LDR image, and $\mathrm{IT_a}[\cdot]$ and $\mathrm{IT_b}[\cdot]$ are ITMO of each method. The modified PSNR [31] between $A \times B$ sized HDR images is given by

$$PSNR = 20\log_{10}(DR) - 10\log_{10}(MSE), \tag{30}$$

$$MSE = \frac{1}{AB}\sum_{p=1}^{AB}[I_{\mathrm{HDR}}(p) - I'_{\mathrm{HDR}}(p)]^2, \tag{31}$$

$$DR = max(I_{\mathrm{HDR}}(p)) - min(I_{\mathrm{HDR}}(p)). \tag{32}$$

The HDR-VDP-2.2 takes a value from 0 to 100. The lager score indicates a higher similarity between two images.

Table 2 shows that the results of this experiment. The high average PSNR value and HDR-VDP-2.2 score were obtained with the proposed method. Therefore, the proposed method performed the ITMO maintaining the structural similarity. From the above result, it was confirmed that the proposed method can execute the ITMO with high accuracy, even though it is conducted with the fixed-point arithmetic.

Table 2. The PSNR and HDR-VDP-2.2 values.

	Average value
Modified PSNR	52.66 dB
HDR-VDP-2.2	69.14

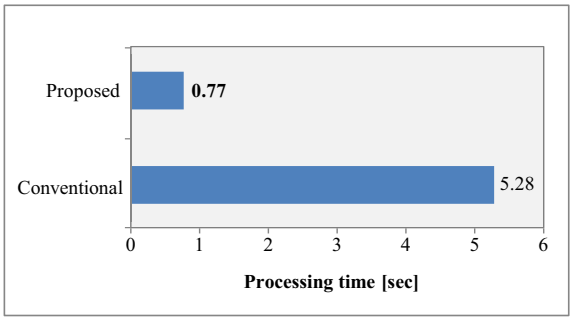

Fig. 5. The processing time of the methods.

4.2. Comparison of the Processing Time

This experiment applied inverse tone mapping for an LDR image with 512×768 pixels using the proposed method and the conventional method, and measured the processing time of the methods. The experimental environment was with Marvell PXA270 ARM Processor 624MHz and 128MB RAM. Note that this processor does not have a FPU.

Figure 5 compares the processing time of the proposed method and the conventional method [24]. The proposed method was 6.86 times faster than the conventional method. Therefore, this experiment confirmed that the proposed method reduced the computational cost by using fixed-point arithmetic.

4.3. Evaluation of the Memory Usage

In software implementation, IEEE754 [3] single-precision format (32-bit) or double-precision format (64-bit) is generally used as floating-point data. In this experiment, the conventional method used the 64-bit double-precision format to store in-processing data.

On the other hand, the proposed method uses two 8-bit integer format (16-bit) to store data. Therefore, the memory usage is reduced by 75% in the proposed method. Similary, it is reduced by 50% against the case of using single-precision format.

5. CONCLUSION

This paper proposed the inverse tone mapping operation with low computational cost. The method can apply the inverse tone mapping to two 8-bit integer numbers which correspond to the exponent part and the mantissa part, separately. Furthermore, the method can be implemented with only fixed-point arithmetic to reduce the computational cost. As a result, the method is effective on a processor without FPU. The experimental results confirmed that the proposed method can execute the ITMO with high accuracy, even though it is with fixed-point arithmetic and integer data.

6. REFERENCES

[1] F. Kainz, R. Bogart, and D. Hess, "The Openexr Image File Format," *ACM SIGGRAPH Technical Sketches*, 2003.

[2] G. Ward, "Real Pixels," Graphics Gems 2., pp.80–83, San Diego, CA, USA: Academic Press, 1992.

[3] "Information technology - Microprocessor Systems - Floating-Point arithmetic," ISO/IEC/IEEE 60559, 2011.

[4] E. Reinhard, M. Stark, P. Shirley, and J. Ferwerda, "Photographic Tone Reproduction for Digital Images," *ACM Trans. Graphics*, Vol.21, No.3, pp.267–276, July. 2002.

[5] E. Reinhard, G. Ward, S. Pattanaik, P. Debevec, W. Heidrich, and K. Myszkowski, "High Dynamic Range Imaging - Acquisition, Display and Image based Lighting," Morgan Kaufmann, 2010

[6] F. Drago, K. Myszkowski, T. Annen, and N. Chiba, "Adaptive logarithmic mapping for displaying high contrast scenes," *Computer Graphics Forum*, Vol.22, pp.419–426, 2003.

[7] R. Fattal, D. Lischinski, and M. Werman, "Gradient Domain High Dynamic Range Compression," *ACM Trans. Graphics*, Vol.21, No.3, pp.249–256, July. 2002.

[8] Y. Zhang, E. Reinhard, and D. Bull, "Perception-based high dynamic range video compression with optimal bit-depth transformation," *Proc. IEEE ICIP*, pp.1321–1324, 2011.

[9] M. Iwahashi and H. Kiya, "Efficient Lossless Bit Depth Scalable Coding for HDR Images," *Proc. APSIPA ASC*, no.OS.49–IVM.17–5, Dec. 2012.

[10] R. Xu, S. N. Pattanaik, and C. E. Hughes, "High-Dynamic-Range Still Image Encoding in JPEG2000," *IEEE Trans. Computer Graphics and Applications*, Vol.25, No.6, pp.57-64, Nov. 2005.

[11] G. Ward, M. Simmons, "JPEG-HDR: a backwards-compatible, high dynamic range extension to JPEG," *ACM SIGGRAPH Courses*, No.3, Jul. 2006.

[12] T. Murofushi, M. Iwahashi, and H. Kiya, "An Integer Tone Mapping Operation for HDR Images Expressed in Floating Point Data," *Proc. IEEE ICASSP*, pp.2479–2483, May 2013.

[13] T. Murofushi, T. Dobashi, M. Iwahashi, and H. Kiya, "An Integer Tone Mapping Operation for HDR Images in OpenEXR with Denormalized Numbers," *Proc. IEEE ICIP*, no.TEC–P10.6, Oct. 2014.

[14] T. Dobashi, A. Tashiro, M. Iwahashi, and H. Kiya, "A fixed-point implementation of tone mapping operation for HDR images expressed in floating-point format," *APSIPA Trans. Signal and Info. Process.*, vol.3, no.e11, pp.1-11, Oct. 2014.

[15] J. Duan, and G. Qiu, "Fast tone mapping for high dynamic range images," *Proc. ICPR*, Vol.2, pp.847–850, Aug. 2004.

[16] M. Slomp, and M. M. Oliveria, "Real-Time Photographic Local Tone Reproduction Using Summed-Area Tables," *Computer Graphics International*, pp.82-91, 2008.

[17] Q. Tian, J. Duan, and G. Qiu, "GPU-accelerated local tone-mapping for high dynamic range images," *Proc. IEEE ICIP*, pp.377–380, Oct. 2012.

[18] T. Dobashi, M. Iwahashi, and H. Kiya, "A Fixed-Point Local Tone Mapping Operation for HDR Images," *Proc. EURASIP EUSIPCO*, pp.933-937, Aug. 2016.

[19] N. Banic and S. Loncaric, "Puma: A High-Quality Retinex-Based ToneMapping Operator," *Proc. EURASIP EUSIPCO*, pp.943-947, Aug. 2016.

[20] F. Banterle, P. Ledda, K. Debattista, and A. Chalmers, "Inverse tone mapping," *Proc. ACM GRAPHITE 2006*, pp.349–356, Nov. 2006.

[21] T. H. Wang, C. W. Chiu, W. C. Wu, J. W. Wang, C. Y. Lin, C. T. Chiu, and J. J. Liou "Pseudo-Multiple-Exposure-Based Tone Fusion With Local Region Adjustment," *IEEE Trans. on Multimedia*, Vol.17, No.4, pp.470–484, 2015.

[22] B. Masia, S. Agustin, R. W. Fleming, O. Sorkine, and D. Gutierrez, "Evaluation of reverse tone mapping through varying exposure conditions," *ACM Trans. on Graphics (TOG)*, Vol.28, p.160, 2009.

[23] A.G. Rempel, M. Trentacoste, H. Seetzen, H.D. Young, W. Heidrich, L. Whitehead, and G. Ward, "Ldr2hdr: on-the-fly reverse tone mapping of legacy video and photographs," *ACM Trans. on Graphics (TOG)*, Vol.26, p.39, 2007.

[24] Y. Kinoshita, S. Shiota, and H. Kiya, "FAST INVERSE TONE MAPPING WITH REINHARDS GLOBAL OPERATOR," *Proc. IEEE ICASSP*, pp.19721976, March 2017.

[25] "Information technology – Scalable compression and coding of continuous-tone still images –," ISO/IEC 18477-1, Jun. 2015.

[26] M. Le Pendu, C. Guillemot, and D. Thoreau, "Local inverse tone curve learning for high dynamic range image scalable compression," *IEEE Trans. Image Processing*, Vol.24, No.12, pp.5753–5763, 2015.

[27] M. Iwahashi and H. Kiya, "Two Layer Lossless Coding of HDR Images," *Proc. IEEE ICASSP*, pp.1340-1344, May 2013.

[28] M. Iwahashi, T. Yoshida, N. B. Mokhtar, and H. Kiya, "it-Depth Scalable Lossless Coding for High Dynamic Range Images," *EURASIP Journal on Advances in Signal Processing*, no.2015:22, March 2015.

[29] C. H. Lampert, and O. Wirjadi, "Anisotropic Gaussian Filtering Using Fixed Point Arithmetic," *Proc. IEEE ICIP*, pp.1565–1568, Oct. 2006.

[30] K. J. Hass, "Synthesizing Optimal Fixed-Point Arithmetic for Embedded Signal Processing," *Proc. IEEE MWSCAS*, pp.61–64, Aug. 2010.

[31] S. Choi, O. Kwon, D. Jang, and S. Choi "Performance Evaluation of JPEG XT Standard for High Dynamic Range Image Coding," *Proc. the World Congress on Engineering (WCE)*, pp.552–556, Jul. 2015.

[32] M. Narwaria, R. K. Mantiuk, M. P. Da Silva, and P. Le Callet, "Hdr-vdp-2.2: a calibrated method for objective quality prediction of high-dynamic range and standard images," *Journal of Electronic Imaging*, vol. 24, no. 1, 2015.